

# Exfoliated graphene nanoplatelet cement-based nanocomposites as piezoresistive sensors: influence of nanoreinforcement lateral size on monitoring capability

Zoi S. Metaxa\*

Laboratory of Structural Mechanics, School of Rural and Surveying Engineering, National Technical University of Athens, Zografou Campus, 9 Heroon Polytechniou St, 15780 Athens, Greece

## Abstract

To address the need for innovative multifunctional cement-based materials, this article presents the development of cementitious nano-reinforced composites that exhibit piezoresistive characteristics. It is envisioned that the smart cement-based nanocomposites can be employed as construction materials and at the same time function as stress/strain sensors. To achieve this goal, exfoliated graphene nanoplatelets (xGnPs) were exploited as conductive reinforcement in cement paste. The xGnPs prior to their introduction to the matrix were disentangled using a superplasticizer as dispersant agent and applying ultrasonic energy. The piezoresistive response of the cement-based nanocomposites was assessed by monitoring their electrical resistance change as a function of the applied stress under monotonic compressive as well as flexural tests. The potential of the xGnP cementitious nanocomposites to be used as piezoresistive sensors is demonstrated by the observed linearity between the electrical resistance change values and the respective applied mechanical stress. The effect of the xGnPs lateral size on the monitoring sensitivity of the cement-based nanocomposites was experimentally studied. It is confirmed that the morphology of the nanoplatelets strongly affects the self-sensing performance of the nanocomposites. The xGnPs with the largest lateral size demonstrated an increased change in the electrical resistance proving to be more suitable for improving the monitoring capability of the nanocomposite.

© 2016 Portuguese Society of Materials (SPM). Published by Elsevier España, S.L.U. All rights reserved.

*Keywords:* cement-based nanocomposites; exfoliated graphene nanoplatelets; piezoresistive characteristics.

## 1. Introduction

Monitoring the structural integrity of the infrastructure has become of primary importance in civil engineering applications. Real-time monitoring of structures can fulfill the need for safer infrastructure reducing at the same time both maintenance and repair costs. Current technologies to address this issue typically involve the implementation of strain sensors that are placed to the external surface of the structure. The traditional strain gauges, however, provide information only at designated locations of the structure and at particular directions. Cracking and damage can severely alter the

performance of cementitious materials making the development of innovative ways to monitor their structural health a necessity.

Nanotechnology has recently developed promising nanomaterials with innovative multifunctional characteristics. The employment of carbon nanofillers, such as multi-walled carbon nanotubes (MWCNTs), to produce cement-based nanoengineered composites with smart properties has recently received considerable attention [1-6]. Among the carbon-based nanofillers, single layer graphene is considered to be the stronger material ever measured, having a Young's modulus of around 1 TPa and ultimate strength ~130

\* Corresponding author.

E-mail address: [zmetaxa@central.ntua.gr](mailto:zmetaxa@central.ntua.gr) (Z. Metaxa)

GPa at  $\sim 25\%$  strain [7]. Additionally, it exhibits multifunctional properties, i.e. high electrical conductivity and electrical characteristics independent of its chirality [8-10], which can be explored to facilitate the development of innovative nanocomposites. Furthermore, it can be produced in large quantities from graphite using top down production methods at a much lower cost when compared to other carbon-based nanofillers.

Multiple graphene sheets, typically referred as graphene nanoplatelets (GNPs), can be produced from pristine graphite by mechanical and chemical exfoliation methods [11-13]. The GNPs are composed of few graphene layer stacks having a thickness of 1 to 100 nm. They demonstrate remarkable physical, mechanical and electrical properties [14], are commercially available in large quantities and represent a cost-effective option compared to MWCNTs.

Currently, research on the GNPs exploitation as embedded sensor in cementitious matrices is limited. The potential of using the GNPs as conductive filler in cement-based materials was firstly studied by Sedaghat et al [15]. They investigated the electrical resistivity of cement nanocomposites reinforced with 1, 5 and 10 vol% GNPs, proving that the GNPs can be used to decrease the resistivity of the cementitious matrix. The possibility of using the cement/GNPs nanocomposites as sensors was demonstrated initially by Pang et al [16]. They investigated the sensing capability of mortar specimens with GNPs under both cyclic and monotonic compressive and tensile loadings. More recently, Le et al [17] studied the damage sensing capability of mortar samples with graphene nanoplatelets at high concentrations (i.e. 1.2 %, 2.4 %, 3.6 % and 4.8 % by volume of the material). Using the four-probe set-up, the electric potential across prismatic specimens with a known notch depth was measured and the results were compared with finite element simulations. No mechanical load was applied. It was demonstrated that as the GNP amount exceeds a percolation threshold value (around 2.4 vol%), the electrical conductivity of the GNP-infused mortar is insensitive to the moisture content, which makes it a reliable damage-sensing material for infrastructure applications.

In this study, cement-based nanocomposites reinforced with exfoliated graphene nanoplatelets (xGNPs) were developed. The goal was to study their piezoresistive characteristics with the potential to produce unique cementitious nanocomposites with self-sensing

capabilities. The xGNPs were dispersed in an aqueous solution containing a commercially available superplasticizer. Ultrasonication with a probe homogenizer was engaged to disperse the xGNPs in the suspension prior to mixing with cement. The capability of three different xGNPs, having the same thickness but different lateral sizes / dimensions, namely 5, 15 and 25  $\mu\text{m}$ , was investigated in order to provide efficient stress sensing at the macroscopic scale. The self-sensing behavior of the nanocomposites was explored via monitoring their electrical resistance response under quasi-static monotonic compression as well as flexural tests.

## 2. Experimental Details

### 2.1. Materials

Type I ordinary Portland cement was used to produce the GNPs/cement paste nanocomposites. The exfoliated graphene nanoplatelets (xGNPs) were supplied by XG sciences Inc, Michigan. Grade M xGNPs, having an average thickness of approximately 6 – 8 nm and a typical surface area of 120 to 150  $\text{m}^2/\text{g}$ , were chosen because they have been shown to improve the electrical and electromechanical properties of polymer matrices [18-21]. The xGNPs characteristics are shown in Table 1. Three different xGNP types having the same physical and mechanical characteristics, the same thickness but different lateral size (diameter), namely 5, 15 and 25  $\mu\text{m}$ , were used. To facilitate with the xGNPs dispersion in an aqueous suspension, a superplasticizer based on polycarboxylate polymers, provided by Sika Hellas with the commercial name ViscoCrete® Ferro 1000 was used. This particular dispersant type was employed as it has been shown to be the most effective in dispersing the xGNPs for cementitious materials [22].

Table 1. Exfoliated graphene nanoplatelets properties [23].

	Parallel to surface	Perpendicular to surface
Density ( $\text{g}/\text{cm}^3$ )		2.2
Carbon content (%)		>99.5
Tensile Modulus (GPa)	1000	N/A
Tensile Strength (GPa)	5	N/A
Electrical Conductivity (S/m)	$10^7$	$10^2$

## 2.2. Production of the xGnP/cement based nanocomposites

The xGnPs prior to their introduction to the cementitious matrix were disentangled/homogeneously dispersed in an aqueous solution through the aid of a superplasticizer and ultrasonic energy application. To ensure that the xGnPs were dispersed in a similar manner, the proportions of the water/admixture/xGnP per volume were kept constant in the suspensions at approximately 70 vol%, 28.3 vol% and 1.7 vol%, respectively, regardless the xGnPs type used. Three different aqueous / xGnPs suspensions were prepared, one for each xGnP type studied. To facilitate easy handling and adaptation of the xGnPs suspensions in the field, the volume of the suspensions was kept low by using a minimum amount of water that corresponded to 6 % of the mixing water for the case of 5  $\mu\text{m}$  xGnPs and 9 % of the mixing water for the case of 15 and 25  $\mu\text{m}$  xGnPs. A constant superplasticizer to xGnPs weight ratio of 8.0 was used in all the dispersions. Ultrasonic energy was applied to the suspensions through a probe ultrasonicator that operated at 50 % of its power and at cycles of 0.5 s to prevent overheating of the suspensions.

Based on the authors' previous research [24], the xGnPs concentration affect the electrical resistivity of the cementitious matrix. The optimal concentration of xGnPs with a small size (average diameter of 5  $\mu\text{m}$ ) was found to be around 0.1 wt% of cement. In the case of xGnPs with a larger diameter (average diameters of 15 and 25  $\mu\text{m}$ ) a slightly higher concentration, around 0.15 wt% of cement, was found to be optimum. These optimum concentrations were defined based on the electrical resistivity response of the xGnP cement-based nanocomposites as these particular samples demonstrated the lowest electrical resistivity. One of the objectives of this research was to study the piezoresistive characteristics of these cement-based nanocomposites. Therefore, cementitious nanocomposites reinforced with i) 5  $\mu\text{m}$  xGnPs at a concentration of 0.1 wt% of cement, ii) 15  $\mu\text{m}$  xGnPs at an amount of 0.15 wt% of cement and iii) 25  $\mu\text{m}$  xGnPs at a loading of 0.15 wt% of cement, were produced.

After ultrasonic processing, extra water was added to the xGnPs suspensions corresponding to a water to cement ratio of 0.3. The resulting mixture after hand stirring was mixed with the cement powder according to ASTM C305 using a standard mixer. After mixing, the cement paste nanocomposites were cast in prismatic 20×20×80 mm molds. The specimens were demolded

after one day and placed in water saturated with lime until the age of 28 days. Prior to testing, the samples were placed in an electrical heating oven with air circulation at a temperature of  $80 \pm 1^\circ\text{C}$  to dry for 72 h.

## 2.3. Electrical resistance measurements

The electrical resistance of the nanocomposites was measured during mechanical testing using the two and four wire methods for the case of flexural and compression testing, respectively. In the case of the two wire method, two electrical wires were placed at the bottom of the specimens before testing (Fig. 1). To ensure appropriate bonding between the wires and the nanocomposites and transfer of the electrical current, silver conductive paint and paste were used (Fig. 1a). Initially silver paste was applied to the surface of the specimens at the designated contact points having a distance of 15 mm (Fig. 1b). Following, the electrical wiring was installed with the aid of a silver conductive paste (Fig. 1c). Few of the produced nanocomposites with the installed wiring are shown in Fig. 1d. In the case of the four wire method, immediately after casting, four steel electrodes that covered the entire cross-section of the specimens were embedded into the samples (Fig. 2a). The distance between the outer and inner electrodes was 15 mm and the space between the inner electrodes was 30 mm. The inner electrodes were used to measure the voltage and the outer electrodes to supply the direct current. A Keysight multimeter was used for both the two and the four wire ohm measurements. The electrical resistance measurements were recorded every second during the mechanical tests.

## 2.4. Mechanical testing

The piezoresistive behaviour of the produced nanocomposites was studied *in-situ* under monotonic compression and flexure (four point bending – 4pb) tests. The monotonic compression tests were performed at a 300 kN Instron SATEC loading frame. The experimental test set up can be seen in Fig. 2b. The crosshead displacement rate was kept constant and equal to 0.5 mm/min. During testing time, crosshead displacement, mechanical force from the loading frame as well as electrical resistance from the multimeter using the aforementioned four wire method were recorded.

Monotonic flexural tests were performed at a 10 kN MTS Insight testing machine. The four point bending test set up can be seen in Fig. 3a. The two wire method

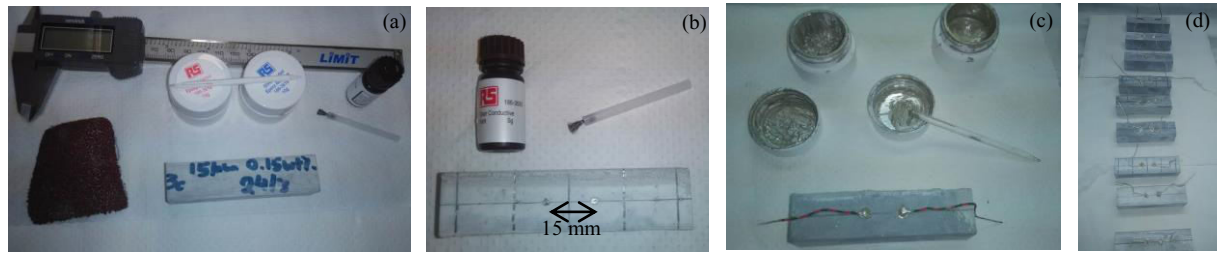


Fig. 1. Specimens preparation for the 2 wire electrical resistance measurements: (a) typical specimen and equipment that was used, (b) silver paint application at the measurement points on the specimen surface, (c) typical specimen with installed electrical wiring and (d) photograph of few specimens before mechanical testing.

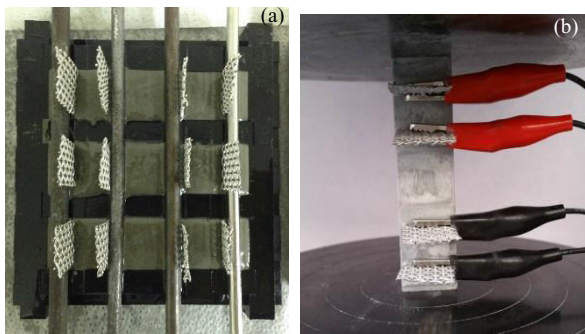


Fig. 2. (a) Specimens with the four steel electrodes immediately after casting that were used for the 4 wire electrical resistance measurements and (b) experimental test set up for the piezoresistivity measurements under compression.

was used to measure the electrical resistance of the nanocomposites. To investigate the piezoresistive capability of the nanocomposites under tensile mechanical loads, the specimens were placed at the testing fixture so as the attached wiring cables to be at the bottom of the samples (Fig. 3b). The span length was set at 70 mm, while the distance between the loading points was 35 mm, half of the span length. The tests were performed using a crosshead displacement rate of 0.008 mm/sec. During testing time, crosshead displacement and mechanical force from the loading frame as well as electrical resistance from the multimeter were recorded.

### 3. Results and Discussion

#### 3.1. Mechanical performance

The average compressive and flexural strength with the standard deviation values of the investigated nanocomposites are depicted in Fig. 4. The compressive strength results are shown in red circles

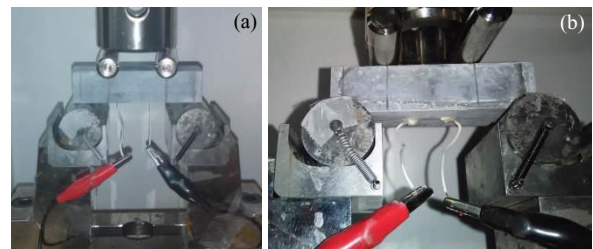


Fig. 3. (a) Experimental test set up for piezoresistivity measurements under four point bending and (b) bottom view and magnification of the specimen showing the electrical wiring.

while the flexural strength results are in black squares. Compared to the reference cement paste, without nanoreinforcement, the nanocomposites demonstrate an up to 49% and 27% increase in the compressive and the flexural strength, respectively. Possibly the graphene nanoplatelets, due to their two dimensional morphology and high surface area, are filling the pores and arresting part of the nano and micro-cracks. The results indicate that the xGnP cement-based nanocomposites can be successfully employed as construction materials.

Comparing the response of the nanocomposites under compression it is observed that they demonstrate a similar behavior. The average compressive strength is around 74 MPa, with the 25  $\mu\text{m}$  xGnPs reinforced samples having more consistent results and a lower scatter. The xGnPs lateral size does not seem to influence the compressive strength of the nanocomposites. On the contrary, small variations at the average strength values under bending, possibly depending on the lateral dimension of the xGnPs, are observed. The nanocomposites reinforced with the larger xGnPs, having a lateral size of 25  $\mu\text{m}$ , demonstrate a slightly higher average flexural strength (6.5 MPa) compared to the other nanocomposites.

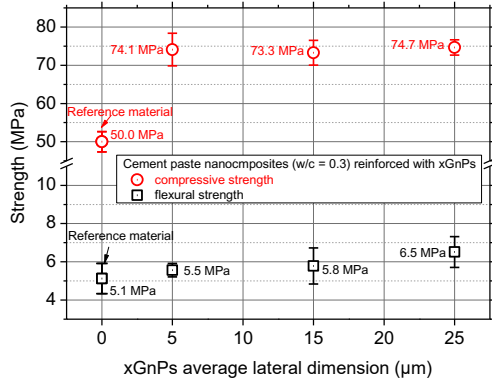


Fig. 4. Effect of xGnPs lateral dimension on the mechanical response of the nanocomposites.

### 3.2. Piezoresistive behavior under compression

The xGnPs/cementitious nanocomposites were subjected to monotonic compression while simultaneously measuring their electrical resistance through the four wire method. The compressive stress (black squares) and the respective change in the electrical resistance (blue lines) versus the crosshead displacement of the nanocomposites reinforced with the xGnPs having three different lateral dimensions can be seen in Fig. 5. The fracture point is clearly marked up in the diagrams. The electrical resistance change of the nanocomposites is observed to be inverse analogous to the applied mechanical stress, e.g. when the mechanical load is increasing the electrical resistance change is decreasing. This is because during loading the xGnPs are coming closer, their interparticle distances are decreasing which results to the observed reduction in the electrical resistance. This response is found to be approximate linear at the beginning of loading (the elastic region of the materials) up until fracture, where an abrupt increase in the electrical resistance change is noticed. Internal cracking of the specimens that leads to the breakage of conductive paths between the xGnPs can explain this sudden increase. After fracture, due to macrocracking, the electrical resistance change keeps increasing. The results are very encouraging and demonstrate the possibility of using the xGnPs for monitoring purposes in cementitious materials.

Comparing the electrical resistance change values at the fracture point, it is obvious that the nanocomposites reinforced with the smaller xGnPs (5 µm) provide the lower  $\Delta R/R_0$ , approximately -2.4 %. The 15 µm xGnP nanocomposites demonstrate a slightly larger value ( $\Delta R/R_0 \sim -2.65$  %). The xGnPs / cement nanocomposites with the largest lateral dimension (25 µm) exhibit the optimum behavior with a resistance

change that reaches  $\Delta R/R_0 \sim -4$  %. The lateral size of the xGnPs is found to play an important role on their sensing capability. The xGnPs with the largest lateral dimension examined provide the cementitious nanocomposite with better screening capability for the same compressive stress / strain state.

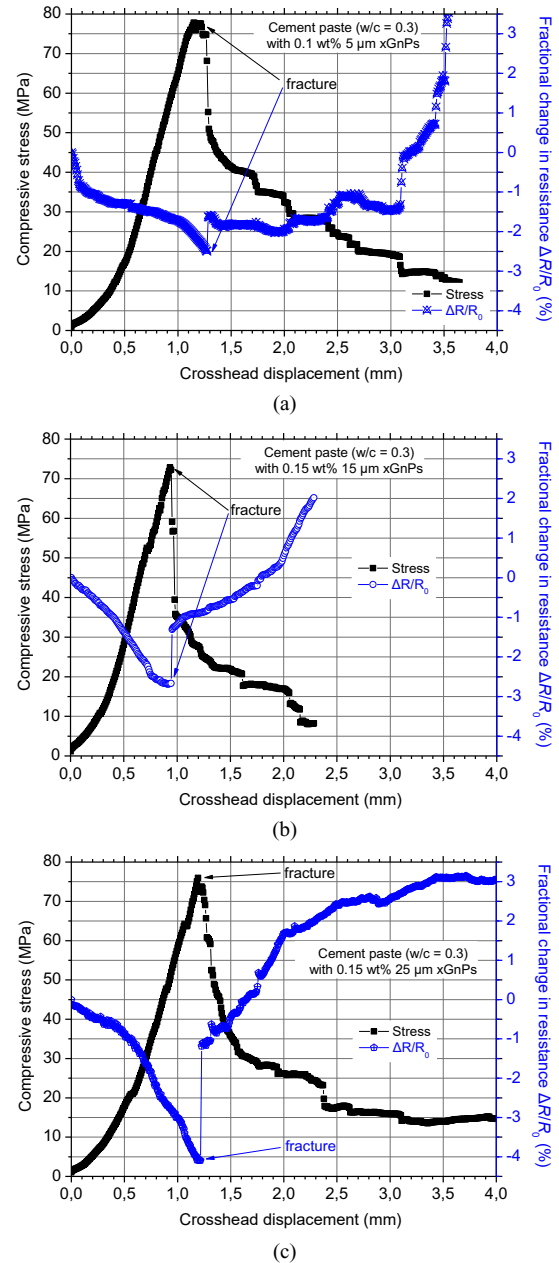


Fig. 5. Compressive stress and fractional electrical resistance change over crosshead displacement of the investigated nanocomposites reinforced with xGnPs having a lateral size of: (a) 5 µm, (b) 15 µm and (c) 25 µm.

### 3.3. Piezoresistive behavior under flexure

The xGnPs/cementitious nanocomposites were also subjected to monotonic four point bending while simultaneously measuring their electrical resistance. The two wire method, described in the experimental procedure, was employed with the objective to monitor the electrical resistance change at the lower surface of the specimen that is subjected to a uniform bending moment under tension. The results of the flexural stress (black squares) and the fractional change in the electrical resistance (blue lines) versus testing time of the nanocomposites reinforced with the three different xGnPs are shown in Fig. 6. The fractional change in the electrical resistance of the nanocomposites is increasing linearly and is analogous to the applied flexural stress up till fracture. During loading the interparticle distance between the xGnPs at the tensile face of the specimen is increasing. As a result some of the electrical paths are ‘disrupted / broken’ and consequently the electrical resistance of the nanocomposites is increasing. At fracture, a sudden increase in electrical resistance change for all nanocomposites is observed that coincides with the sudden drop in the mechanical load. The observed increase in the electrical resistance beyond the fracture point can be correlated with the disruption of the conductive paths due to cracking.

The fractional change in electrical resistance at fracture, similar to the monotonic compression results, seems to depend on the xGnP type. For the nanocomposites with the lowest xGnP lateral dimension (5  $\mu\text{m}$ ) a fractional change of around  $\Delta R/R_0 = 1\%$  was recorded at fracture. The respective  $\Delta R/R_0$  value is increasing dramatically ( $\Delta R/R_0 \sim 2.75\%$ ) when xGnPs with three times larger lateral size (15  $\mu\text{m}$ ) are used. The optimum results, similar to the monotonic compression results reported earlier and previous results on cyclic compression in the elastic region [24], are obtained with the xGnPs having the largest lateral dimension (25  $\mu\text{m}$ ). A fractional change in the electrical resistance close to 3% is observed at fracture. The results strongly demonstrate that the self-sensing performance of the nanocomposites strongly depends on the morphology of the reinforcement, i.e. their lateral dimension. The xGnPs having the largest lateral size, among the three different types studied, were found to be more suitable to develop cementitious nanocomposites for monitoring applications as they presented improved monitoring capability.

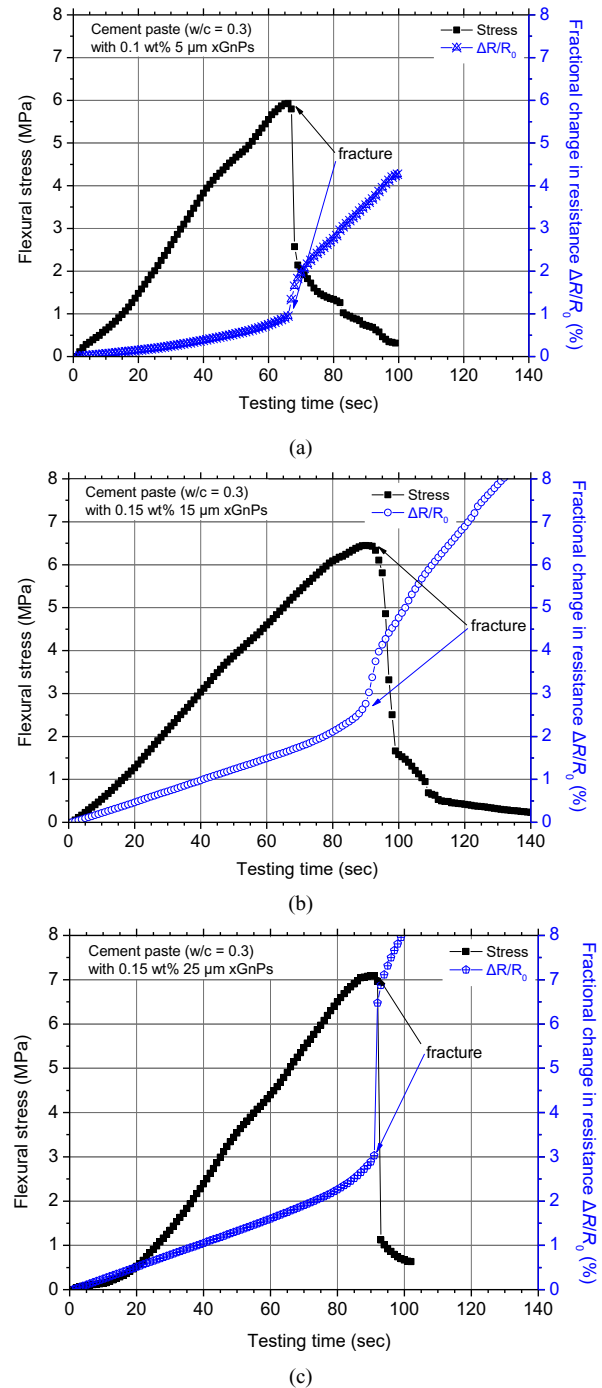


Fig. 6. Flexural stress and fractional electrical resistance change over testing time of the investigated nanocomposites reinforced with xGnPs having a lateral size of: (a) 5  $\mu\text{m}$ , (b) 15  $\mu\text{m}$  and (c) 25  $\mu\text{m}$ .

#### 4. Conclusions

The potential of using exfoliated graphene nanoplatelets (xGnPs) as conductive reinforcement in cementitious materials with the objective to develop novel cement based nanocomposites with piezoresistive characteristics was investigated. During compression, the resistance change of the nanocomposites was found to be inversely analogous to the applied stress. Due to the reduction of the xGnPs interparticle distance, the resistance of the nanocomposites decreases up until the maximum compressive load. During bending, the electrical response of the nanocomposites was found to be analogous to the applied stress up until fracture. The interparticle distance between the xGnPs at the tensile face of the specimen is increasing therefore part of the conductive paths are disrupted and consequently the electrical resistance change of the nanocomposites is increasing.

The sensing sensitivity of the nanocomposites was studied as a function of the different xGnPs lateral dimensions. The addition of the xGnPs improved the mechanical performance of the matrix. It was found that the xGnPs lateral size does not seem to influence the compressive strength of the nanocomposites. On the contrary, the flexural strength slightly increases with increasing the xGnPs lateral size. It was confirmed that the self-sensing performance of the nanocomposites strongly depends on the morphology of the nanoplatelets, i.e. their lateral size. The monitoring capability of the nanocomposites was improved with increasing the xGnPs lateral dimension. In general, the linearity of the electrical resistance change of the nanocomposites according to the applied stress, under both compression and flexure, demonstrates the viability of the xGNP cementitious nanocomposites to be used as piezoresistive sensors. Consequently, the xGnPs can offer great advantages as multifunctional conductive reinforcements of cementitious materials for structural health monitoring applications.

#### Acknowledgements

The author would like to acknowledge the financial support of IKY fellowships of excellence for postgraduate studies in Greece – Siemens Program.

#### References

- [1] G.Y. Li, P.M. Wang, X. Zhao, *Cement Concrete Comp.* 29 (2007) 377.
- [2] X. Yu, E. Kwon, *Smart Mater. Struct.* 18 (2009) 5.
- [3] M. Saafi, *Nanotechnology*, 20 (2009) 395502.
- [4] L. Coppola, A. Buoso, F. Corazza, *Appl. Mech. Mater.* 82 (2011) 118.
- [5] B. Han, K. Zhang, X. Yu, E. Kwon, J. Ou, *Cement Concrete Comp.* 34 (2012) 794.
- [6] M.S. Konsta-Gdoutos, C.A. Aza, *Cement Concrete Comp.* 53 (2014) 162.
- [7] C. Lee, X. Wei, J. Kysar, J. Hone, *Science*, 321, (2008) 385.
- [8] X. Du, I. Skachko, A. Barker, E.Y. Andrei, *Nat. nanotechnol.* 3 (2008) 491.
- [9] M. Pumera, *Chem. Soc. Rev.* 39 (2010) 4146.
- [10] Z. Yang, R. Gao, N. Hu, J. Chai, Y. Cheng, L. Zhang, H. Wei, E. S.-W. Kong, Y. Zhang, *Nano-Micro Lett.* 3 (2011) 272.
- [11] J. Hass, W.A. de Heer, E.H. Conrad, *J. Phys. Condens. Matter.* 20 (2008) 323202.
- [12] S. Park, R.S. Ruoff, *Nat. Nanotechnol.* 4 (2009) 217.
- [13] S.D. Bergin, Z. Sun, D. Rickard, P.V. Streich, J.P. Hamilton, J.N. Coleman, *ACS Nano*, 3 (2009) 2340.
- [14] B.Z. Jang, A. Zhamu A, *J. Mater. Sci.* 43 (2008) 5092.
- [15] A. Sedaghat, M. Ram, A. Zayed, R. Kamal, N. Shanahan, *Open J. Compos. Mater.* 4 (2014) 12.
- [16] S.D. Pang, H.J. Gao, C. Xu, S.T. Quek, H. Du, *Proceedings of SPIE vol. 9061, Sensors and Smart Structures Technologies for Civil, Mechanical, and Aerospace Systems 2014*, 906126 (Eds. J.P. Lynch, K.-W. Wang, H. Sohn), San Diego, California, USA, March 2014 (doi:10.1117/12.2045329).
- [17] J.-L. Le, H. Du, S.D. Pang, *Compos. Part B-Eng.* 67 (2014) 555.
- [18] S. Chatterjee, F.A. Nuesch, B.T.T. Chu, *Nanotechnology*, 22 (2011) 275714.
- [19] A. Das, G.R. Kasaliwal, R. Jurk, R. Boldt, D. Fischer, K.W. Stöckelhuber, G. Heinrich, *Compos. Sci. Technol.* 72 (2012) 1961.
- [20] J.-M. Park, G.-Y. Gu, Z.-J. Wang, D.-J. Kwon, K.L. DeVries, *Thin Solid Films*, 539 (2013) 350.
- [21] S.-H. Hwang, H.W. Park, Y.-B. Park, M.-K. Um, J.-H. Byun, S. Kwon, *Compos. Sci. Technol.* 89 (2013) 1.
- [22] Z.S. Metaxa, *J. Eng. Sci. Technol. Rev.* 8 (5) (2015) 1.
- [23] xGNP® Graphene Nanoplatelets, Technical Data Sheet, 2013.
- [24] Z.S. Metaxa, In *Proceedings of 20<sup>th</sup> International Conference on Composite Materials (ICCM20)*, Copenhagen, 2015.